Accepted Manuscript

Title: Impact of Fe(III) as an effective electron-shuttle mediator for enhanced Cr(VI) reduction in microbial fuel cells: Reduction of diffusional resistances and cathode overpotentials

Author: Qiang Wang Liping Huang Yuzhen Pan Xie Quan Gianluca Li Puma

PII: S0304-3894(16)30908-6
DOI: http://dx.doi.org/doi:10.1016/j.jhazmat.2016.10.011
Reference: HAZMAT 18092

To appear in: *Journal of Hazardous Materials*

Received date: 9-7-2016
Revised date: 9-9-2016
Accepted date: 5-10-2016

Please cite this article as: Qiang Wang, Liping Huang, Yuzhen Pan, Xie Quan, Gianluca Li Puma, Impact of Fe(III) as an effective electron-shuttle mediator for enhanced Cr(VI) reduction in microbial fuel cells: Reduction of diffusional resistances and cathode overpotentials, Journal of Hazardous Materials http://dx.doi.org/10.1016/j.jhazmat.2016.10.011

This is a PDF file of an unedited manuscript that has been accepted for publication. As a service to our customers we are providing this early version of the manuscript. The manuscript will undergo copyediting, typesetting, and review of the resulting proof before it is published in its final form. Please note that during the production process errors may be discovered which could affect the content, and all legal disclaimers that apply to the journal pertain.

ACCEPTED MANUSCRIPT

September 9, 2016

Submitted to Journal of Hazardous Materials R1

Impact of Fe(III) as an effective electron-shuttle mediator for enhanced Cr(VI) reduction in microbial fuel cells: Reduction of diffusional resistances and cathode overpotentials

Qiang Wang[1], Liping Huang[1,*], Yuzhen Pan[2], Xie Quan[1], Gianluca Li Puma[3,,*]

1. Key Laboratory of Industrial Ecology and Environmental Engineering, Ministry of Education (MOE), School of Environmental Science and Technology, Dalian University of Technology, Dalian 116024, China

2. College of Chemistry, Dalian University of Technology, Dalian 116024, China

3. Environmental Nanocatalysis & Photoreaction Engineering, Department of Chemical Engineering, Loughborough University, Loughborough LE11 3TU, United Kingdom

Corresponding authors:

(L. Huang) lipinghuang@dlut.edu.cn Tel./Fax.: 86 411 84708546

(G. Li Puma) g.lipuma@lboro.ac.uk Tel.: 44 1509263171

ACCEPTED MANUSCRIPT

Graphical abstract

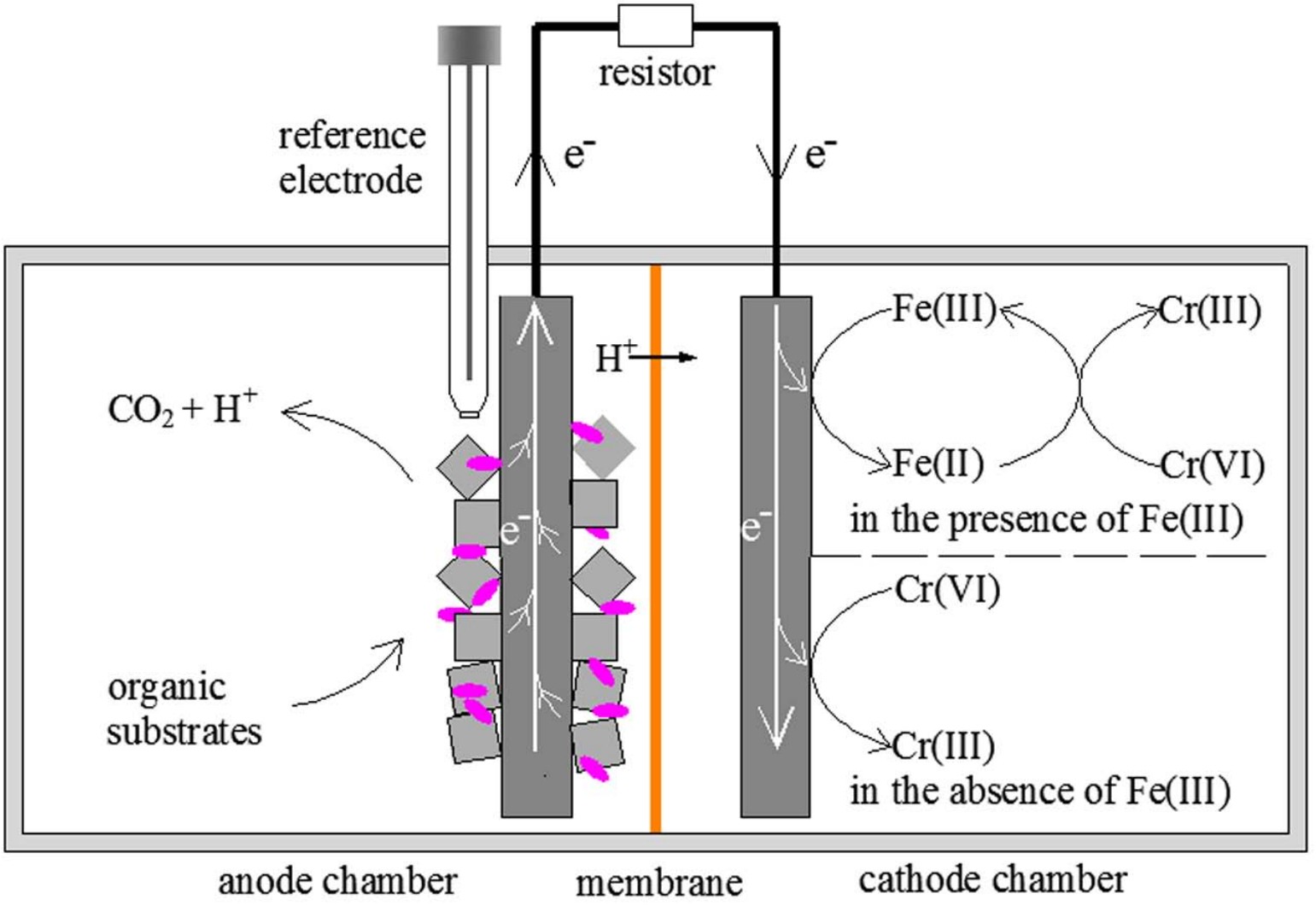
resistor
reference electrode
e-
e-
H+
CO2 + H+
e-
e-
Fe(III)
Cr(III)
Fe(II)
Cr(VI)
in the presence of Fe(III)
Cr(VI)
organic substrates
Cr(III)
in the absence of Fe(III)
anode chamber
membrane
cathode chamber

ACCEPTED MANUSCRIPT

Highlights

Fe(III) shuttles electrons for enhanced reduction of Cr(VI) in MFCs;

The coulombic efficiency increases by 1.6 fold in the presence of Fe(III);

The reduction of Cr(VI) occurs via an indirect Fe(III) mediation mechanism;

Fe(III) decreases the diffusional resistances and the cathode overpotentials.

ACCEPTED MANUSCRIPT

Abstract

The role of Fe(III) was investigated as an electron-shuttle mediator to enhance the reduction rate of the toxic heavy metal hexavalent chromium (Cr(VI)) in wastewaters, using microbial fuel cells (MFCs). The direct reduction of chromate (CrO_4^-) and dichromate ($Cr_2O_7^{2-}$) anions in MFCs was hampered by the electrical repulsion between the negatively charged cathode and Cr(VI) functional groups. In contrast, in the presence of Fe(III), the conversion of Cr(VI) and the cathodic coulombic efficiency in the MFCs were 65.6% and 81.7%, respectively, 1.6 times and 1.4 folds as those recorded in the absence of Fe(III). Multiple analytical approaches, including linear sweep voltammetry, Tafel plot, cyclic voltammetry, electrochemical impedance spectroscopy and kinetic calculations demonstrated that the complete reduction of Cr(VI) occurred through an indirect mechanism mediated by Fe(III). The direct reduction of Cr(VI) with cathode electrons in the presence of Fe(III) was insignificant. Fe(III) played a critical role in decreasing both the diffusional resistance of Cr(VI) species and the overpotential for Cr(VI) reduction. This study demonstrated that the reduction of Cr(VI) in MFCs was effective in the presence of Fe(III), providing an alternative and environmentally benign approach for efficient remediation of Cr(VI) contaminated sites with simultaneous production of renewable energy.

Keywords: Cr(VI) reduction; Fe(III) mediator; diffusion resistance; cathode overpotential; microbial fuel cell

ACCEPTED MANUSCRIPT

1 Introduction

The heavy metal hexavalent chromium (Cr(VI), as $Cr_2O_7^{2-}$ or CrO_4^- in solution) typically found in the wastewaters from the electroplating and mining industries, is known to be extremely toxic and carcinogenic to living organisms when discharged to the environment [1]. The reduction of Cr(VI) to the less toxic Cr(III) is a feasible and common method for Cr(VI) removal in contaminated sites [1-2]. Conventional methods for Cr(VI) reduction include chemical, physicochemical, electrochemical and biological processes [1-2]. Recently, microbial fuel cells (MFCs) have also shown promising results for the reduction of Cr(VI) since they couple reduced sludge generation with the production of renewable energy [3-4]. In MFCs, electrons are released from reductive organic matters in the anode in the presence of exoelectrogens. These electrons flow to the cathode, where they are captured by reductive species such as dissolved oxygen or metal ions, producing renewable energy in the form of electricity. The reduction of Cr(VI) and the generation of electricity in MFCs have been reported in literature with variable degrees of success (Table 1), using different solution conditions, reactor architectures and cathode electrodes. However, since the Cr(VI) species ($Cr_2O_7^{2-}$ or CrO_4^{2-}) are electronegative and mutually exclusive against the negatively charged cathodes, the reduction of Cr(VI) and the electrochemical reaction kinetics are usually slow. The development of biocathodes based on the electrotrophic mediation between cathode electrode and Cr(VI) [12-13,15-19] appears to be a promising method for the reduction of Cr(VI) in MFCs. However, the challenges include the requirements of maintaining low initial Cr(VI) concentrations and a neutral catholyte environment, limiting its practical

ACCEPTED MANUSCRIPT

application, due to the high concentrations of Cr(VI) usually found in the acidic wastewaters from the electroplating and mining industries. Much effort is still needed to achieve efficient Cr(VI) reduction in MFCs, particularly with regards to promoting the interfacial interactions between the negatively charged cathode surface and the negative functional group of $Cr_2O_7^{2-}$ or CrO_4^{2-}. This aspect is crucial for the scaling-up of this technology.

Here Table 1

Species having the properties of displaying reversible redox reactions to function as electron mediators, are potentially effective to eliminate the electrical repulsion between the negatively charged cathode and $Cr_2O_7^{2-}$ or CrO_4^{2-} anions, and this is essential to achieve enhanced Cr(VI) reduction. Solid-phase mediating species such as rutile TiO_2 under light irradiation or conductive polymers of pyrrole/ClO_4^- and pyrrole/9,10-anthraquinone-2-sulfonate can facilitate the reduction of Cr(VI) in MFCs [5,8]. However, the poor durability of the costly rutile and pyrrole, as well as the undesirable environmental impact due to their dissolution over time may limit these approaches for practical application. Compared to solid mediators, dissolved electron mediators have the merit of reaching appreciable solubilities in aqueous media and thus can rapidly equilibrate the charges with the working electrode and the final electron acceptors [20-21]. In the air cathode MFCs, the in-situ generation of dissolved H_2O_2 mediates the reduction of Cr(VI) [6], although the unfavorable oxygen reduction kinetics substantially affects system performance. An alternative method includes the use of dissolved Fe(III), as an environmentally benign and cost

ACCEPTED MANUSCRIPT

effective mediator in MFCs. Fe(III) promotes the electron transfer between the cathode and either *Acidithiobacillus ferrooxidans* [22-23] or 2-nitrophenol [24] in MFCs. However, the role that Fe(III) could play in decreasing the electrode overpotential has not been investigated and the mechanism of Fe(III) mediation has not been systematically elucidated, particularly with regards to the reduction of Cr(VI). The use of Fe(III) and the exemplification of its role in the enhancement of Cr(VI) reduction is not trivial since Fe(III) often co-exists with Cr(VI) in the wastewaters from the electroplating and mining industries [25].

In general, more efficient MFC performance is favored by lower electrode overpotential and interfacial diffusional resistance. Larger electrode surface areas, more efficient electrode catalysts and higher solution conductivities have been frequently reported to decrease electrode overpotential in MFCs [26-28]. In parallel, diffusional resistance in MFC anodes has been moderated by modification of the anode surface with carbon nanoparticles [29] or with the addition of appropriate amounts of a dye [30]. Whether or not Fe(III) plays an effective mediating role resulting in a decrease in both the diffusional resistance of Cr(VI) species and the overpotential for Cr(VI) reduction in MFCs, is to our knowledge still scarcely reported.

Here Fig. 1

A clarification of the relationships among Fe(III), Cr(VI) and cathode electrons is essential to explain the role of Fe(III) as a mediating species in MFCs. High circuital currents associated with low external resistances can provide an excess of electrons to

ACCEPTED MANUSCRIPT

both the positively charged Fe(III) and the negatively charged $Cr_2O_7^{2-}$ or CrO_4^{2-} anions, highlighting the benefit of electron transfer via Fe(III) mediator (Fig. 1). However, this mechanism cannot exclude the alternative prospect of direct electron transfer between the cathode electrode and $Cr_2O_7^{2-}$ or CrO_4^{2-} ions, due to the somewhat weak repulsive forces between the $Cr_2O_7^{2-}$ or CrO_4^{2-} and the limited cathode electrons. Therefore, the role of these two competing routes for Cr(VI) reduction in MFCs needs to be clarified.

In this study, the role of Fe(III) supplied at different dosages and under various external resistances was systematically explored as a mediating species for enhanced Cr(VI) reduction in MFCs. The system performance was evaluated in terms of Cr(VI) reduction, circuital current and cathodic coulombic efficiency (CE_{ca}). The relationships among Fe(III), Cr(VI) and cathode charge were extensively elucidated by linear sweep voltammetry (LSV), Tafel plot, cyclic voltammetry (CV) and electrochemical impedance spectroscopy (EIS). The role of Fe(III) on the diffusional resistance of Cr(VI) species and the overpotential for Cr(VI) reduction was comprehensively disclosed. This study provides a new insight into the mechanisms controlling electron transfer in MFCs operated for Cr(VI) reduction.

2 Materials and Methods

2.1 Reactor setup

Each MFC was made with two cylindrical cubic-shaped chambers housing the electrodes and separated by a cation exchange membrane (CMI-7000 Membranes

ACCEPTED MANUSCRIPT

International, Glen Rock, NJ). Duplicate reactors were used in all experiments. The operational volumes were 15 mL in the anode and 13 mL in the cathode. The anode was filled with graphite felt (Sanye Co., Beijing, China), and a carbon rod was used as the current collector. The cathode was made with a carbon rod (CR, Chijiu Duratight CarbonCo., China) with a projected surface area of 8 cm^2, which was connected to the circuit using a titanium wire. All materials used here were cleaned as previously described [31] in order to avoid the adverse effects of Cr(VI) reduction products on system performance [32]. The anodic chamber housed a saturated calomel reference electrode (SCE, 241 mV vs. a standard hydrogen electrode, SHE) which monitored the anode potential, with all voltage showed here vs SHE. The reactors were wrapped with aluminum foil to block light irradiation and the possible growth of algae on the anodes.

2.2 Inoculation and operation

The anodes were inoculated with the effluent from acetate-fed MFCs and an equivalent volume of nutrient solution as previously described [33]. The anodic nutrient solution contained (g/L) sodium acetate 1.0, KH_2PO_4 4.4, K_2HPO_4 3.4, NH_4Cl 1.3, KCl 0.78, $MgCl_2$ 0.2, $CaCl_2$ 0.0146, NaCl 0.5, trace vitamins and minerals [34]. The anolyte was replaced daily and the bioanodes were considered to be well-developed when the anode potentials stabilized to −0.2 V (vs. SHE) at least three batch cycles.

Various dosages of Fe(III) (analytical reagent of $FeCl_3 \cdot 6H_2O$, Sigma-Aldrich) of

ACCEPTED MANUSCRIPT

0, 50, 100 and 150 mg/L [25] were added in the reactors operated at an external resistance of 1000 Ω, to investigate the effect of Fe(III) concentration on Cr(VI) reduction. Multiple characterization approaches of LSV, Tafel plot and CV were used to assess the influence of Fe(III) dosage on Cr(VI) reduction. The MFCs were run for an operation period of 16 h with a wider range of Fe(III) dosages of 25, 50, 75, 100, 125 and 150 mg/L, to establish the kinetics of Cr(VI) reduction associated with Fe(III). Different external resistors of 10 Ω, 500 Ω, 1000 Ω, 3000 Ω and 5000 Ω were explored to examine the effect of an external resistance on Cr(VI) reduction. The individual impendency of Cr(VI) reduction at different cathode potentials associated with these different external resistances was analyzed using EIS.

Typical concentrations of Cr(VI) and Fe(III) in the wastewaters from the electroplating and mining industries may vary over a wide range, from 0.4 to 270000 mg/L for Cr(VI) and 1.5 to 250 mg/L for Fe(III) [25]. In consequence, this makes difficulty to select a narrow range of Cr(VI) and Fe(III) concentrations to be used in this study. In contrast, to the studies carried out with abiotic cathodes, typical concentrations of Cr(VI) used with biocathodes in MFCs (Table 1) are typically in the lower range as a result of the potential toxicity exerted by Cr(VI) to the bacteria. Therefore, unless otherwise stated, an initial Cr(VI) of 50 mg/L and a Fe(III) dosage of 150 mg/L together with an external resistance of 1000 Ω were always used in subsequent experiments.

The long-term stability of Fe(III) was assessed by running ten consecutive cycles with each cycle lasting 10 h. At the end of each cycle, 150 μL of Cr(VI) (5 g/L)

ACCEPTED MANUSCRIPT

and 150 μL H_2SO_4 (49 g/L) were added to the cathode compartment using a syringe to produce the same initial Cr(VI) concentration and the same initial pH for the subsequent operation cycle.

Three control runs were operated: the first was run in the presence of Fe(III) under open circuit conditions (OCCs) as a control for Cr(VI) reduction on the electrodes in the absence of current. The second control was run in the absence of Fe(III) in the catholyte in OCCs to exclude the role of both Fe(III) and circuital current on Cr(VI) reduction. In the third control, the redox behaviour of the catholyte in the absence of both Cr(VI) and Fe(III) was analyzed to reflect the role of Cr(VI) and Fe(III) on the electrode reactions. The initial pH of the catholyte during the entire investigation was set to 1.5 to inhibit the precipitation of ferric hydroxide at the highest Fe(III) dosage of 150 mg/L, otherwise observed at 2.0 and 2.5 (see Supplementary Material (SM), Fig. S1). Solution conductivity was invariably regulated to 8.45 mS/cm using K_2SO_4. Unless otherwise stated, each batch cycle operation lasted for 3 h. All catholytes were sparged with ultrapure N_2 for at least 10 min before use and all reactors were run in fed-batch mode at room temperature (22 ± 3 ºC).

2.3. Measurements and calculation

The cathode potentials and voltage across the external resistance were monitored by an automatic data acquisition system (PISO-813, Hongge Co.,Taiwan). Current density and power density were normalized to the cathode project area (A/m^2). The

ACCEPTED MANUSCRIPT

dissolved Cr(VI) and Fe(III) were determined according to standard methods [35]. LSV was conducted using a potentiostat (CHI 770c, Chenhua, Shanghai) at a scan rate of 0.1 mV/s. Cr(VI) reduction at various Fe(III) dosages was also studied using Tafel measurement (CHI 770c, Chenhua, Shanghai) in the range of 0.75 – 0.95 V (vs. SHE) with a scan rate of 1.0 mV/s, based on the open circuital potentials (OCP) of the cathodes. EIS measurements were carried at the frequency of 100 kHz to 0.01 Hz with a sinusoidal perturbation of 5 mV in amplitude. Both Tafel and EIS were conducted in MFCs using the cathode as the working electrode, the anode as the counter electrode, and a SCE electrode placed in the cathode chamber as the reference electrode (241 mV vs. SHE). CV analysis was performed in a three-electrode system consisting of a working electrode (cathode electrode), a counter electrode (a platinum plate), and a SCE reference electrode (241 mV vs. SHE). All potentials shown were corrected to a SHE.

The coulombic efficiency (CE_{ca}) at the cathode was calculated as the ratio of the charges consumed for the reduction of Cr(VI) and the total charges flowing across the MFCs, as shown in Eq. 1:

$$CE_{ca} = \frac{\alpha \mathrm{F} \Delta C_{\mathrm{Cr(VI)}} V_{ca}}{10^3 \mathrm{M}_{\mathrm{Cr}} \sum_{i=1}^{n} I_i \Delta t_i} \quad (1)$$

with $\Delta C_{\mathrm{Cr(VI)}}$ the change of Cr(VI) concentration after 3 h, a (3 mol/mol) the number of electrons required for Cr(VI) reduction, V_{ca} the operational volume of the cathode chamber (L); I_i the circuit current (A), M_{Cr} (52 g/mol) the molecular weight of Cr, F the Faraday's constant (96485 C/mol e), 10^3 the conversion unit (mg/g) and t the

ACCEPTED MANUSCRIPT

operation time of each cycle.

The Tafel equation describing the relationship between the cathodic overpotential and the current density in the high overpotential region [36-37], was expressed as Eq. 2:

$$\eta_{cat} = \frac{RT}{\beta F}\log_{10}\left(\frac{i}{i_0}\right) \quad (2)$$

with η_{cat} the cathodic overpotential (V), R the ideal gas constant (8.31 J/mol K), T the temperature (K), F the Faraday constant (96485 C/mol e^{-1}), β the symmetry factor (a constant reflecting the change of activation energy with cathode potential), i the current density and i_0 the exchange current density, a variable parameter related to the activation energy of cathodic reduction under equilibrium conditions.

3 Results and discussion

3.1 Reduction of Cr(VI)

Here Fig. 2

The reduction of Cr(VI) increased steadily in the presence of Fe(III), reaching 65.6 ± 2.2% with 150 mg/L Fe(III) in 3 h (Fig. 2A), which was 1.6-fold higher than the conversion observed in the absence of Fe(III) (40.7 ± 1.0%). Such result illustrates the significant role played by Fe(III) in mediating the reduction of Cr(VI). Comparing these results with literature, the rate of Cr(VI) reduction (equivalent to 9.4 mg/L/h) observed in this study with 150 mg/L Fe(III) was 8.8 times higher than the rate achieved at a higher initial Cr(VI) of 200 mg/L after 4 h [9], even though reduction rates are expected to increase in proportion to the initial concentration of

ACCEPTED MANUSCRIPT

Cr(VI) [1]. In addition, the rate of Cr(VI) reduction observed in Fig. 2A was more than one order of magnitude higher than those observed at an initial Cr(VI) concentration of 100 mg/L after 150 h [4] and at an initial Cr(VI) concentration of 250 mg/L after 240 h, respectively [7].

The adsorption of Cr(VI) on the cathode ranged from 13.8 ± 1.4 to 15.1 ± 0.1% under OCCs at these Fe(III) doses, demonstrating the negligible effect of Fe(III) on Cr(VI) adsorption, and reflecting the crucial role of the circuital current in Cr(VI) reduction. The average circuital current and CE_{ca} exhibited an increasing trend with the concentration of Fe(III), from 0.22 ± 0.04 mA to 0.32 ± 0.00 mA and from 58.1 ± 1.5% to 81.7 ± 2.8%, respectively (Fig. 2B and Fig. 2C). These results illustrate that the presence of Fe(III) as an electron mediator (i) diverted a higher fraction of electrons from the anode to the cathode and (ii) utilized a higher fraction of cathodic electrons for Cr(VI) reduction. The concentration of Fe(III) in the cathodic chamber decreased approximately from 6.7 ± 0.8% to 11.3 ± 1.3% (Fig. 2D), which was mainly ascribed to the adsorption of Fe(III) species on the cationic exchange membrane separating the chambers, since neither iron species nor Cr(VI) were detected in the anodic chamber during one batch cycle operation. These values were slightly lower than those under OCCs (7.3 ± 1.3% to 12.6 ± 1.7%), since the iron species adsorption and migration in the membrane were reduced by the positive direct electric field. The absence of iron and Cr(VI) species in the anodic chamber during one batch cycle operation, further excluded any potential effects on the electrochemical activity of the anode, confirming their retention on the membrane.

ACCEPTED MANUSCRIPT

3.2 Reduction of diffusional resistance and electrode overpotential

Here Fig. 3

Higher OCPs (Fig. 3A) and power densities (Fig. 3B) were observed at different Fe(III) dosages, compared to the results obtained in the absence of Fe(III), illustrating the role of Fe(III) in reducing the electrode overpotential for Cr(VI) reduction. Voltage output (Fig. 3A) and power density (Fig. 3B) at different Fe(III) dosages similarly decreased sharply with an increase in the current density in the low values region, implying the dominance of a diffusion control mechanism in this system [37]. The value of current density turning into diffusion control increased at higher Fe(III) dosage, from 0.25 A/m^2 (50 mg/L) to 0.28 A/m^2 (150 mg/L), which were higher than 0.22 A/m^2 measured in the absence of Fe(III). The role of Fe(III) in diminishing the diffusional resistance of Cr(VI) species in these MFCs was equivalent to that observed with a concentration of Cr(VI) as high as 2600 mg/L in bioelectrochemical systems operated in the absence of any electron mediator species [9].

The cathodic potentials at different Fe(III) dosages similarly varied much more significantly than the anodic potentials over the current density range investigated (Fig. 3C), implying that the performance of these two-chamber MFCs was controlled by the oxidation-reduction reactions at the cathode rather than at the anode.

3.3 Tafel plot

Here Fig. 4

Here Table 2

ACCEPTED MANUSCRIPT

The MFCs performance was further evaluated with Tafel plots (Fig.4a) and the corresponding active kinetic parameters (Table 2). Higher Fe(III) dosages decreased the diffusional resistance of Cr(VI) species (Fig. 4A) and the electrode overpotential for Cr(VI) reduction (Fig. 4B) at a same current density. This behavior well explained the improved circuital currents (Fig. 2B) and the subsequent Cr(VI) reduction (Fig. 2A) at various Fe(III) dosages.

According to Eq. 2, the Tafel slope ($RT/\beta F$) decreased in the presence of increasing concentrations of Fe(III) (Table 2), consistent with the reduction of the cathode electrode overpotential at constant current density (Fig. 4B). The symmetry factor $\beta = 0.29$ calculated from the Tafel slope in the absence of Fe(III) (Table 2), was slightly lower than the value for oxygen reduction ($\beta = 0.3$) on platinum electrode [36]. At $\beta < 0.5$ the activation energy to bring the electron acceptor to an activated state, required for exchanging electrons with the cathode, is very high [36]. Such low value of β observed in the absence of Fe(III), demonstrates an equivalent difficulty, as for the reduction of oxygen [36], in performing Cr(VI) reduction, despite the higher standard redox potential of 1.33 V for Cr(VI) reduction and 1.23 V for oxygen reduction [38]. The highest β of 0.37 together with an improvement of 70% in the exchange current density was obtained at the highest Fe(III) dosage of 150 mg/L (Table 2). These results strongly illustrate the mediating role of Fe(III) in decreasing the activation energy for the reduction of Cr(VI), which results in enhanced reduction rates in MFCs (Fig. 2A).

ACCEPTED MANUSCRIPT

3.4 Relationships among Cr(VI), Fe(III) and cathode electrons

Here Fig. 5

CV showed that the reductive peak current was lower and the reductive peak potential was more positive in the co-presence of Cr(VI) and Fe(III), compared to the control with Cr(VI) only (Fig. 5A). This result implies the occurrence of indirect reduction of Cr(VI) in the presence of Fe(III) (Fig. 1). The reduction of Cr(VI) on iron electrodes, has been reported to have lower reductive peak currents at higher Cr(VI) concentrations due to the occurrence of a higher rate of chemical reduction of Cr(VI) as a result of the Fe(II) leaching from the iron electrode [2]. The shape of the CV patterns in the co-presence of Cr(VI) and Fe(III) was very similar to that observed with Fe(III) only (Fig. 5A), and this phenomenon was invariably the same at higher Fe(III) dosages of 100 mg/L (Fig. 5B) and 150 mg/L (Fig. 5C). In consequence, Fe(III) at all dosages was overwhelmingly superior to Cr(VI) to directly acquire cathodic electrons, which implies that the reduction of Cr(VI) occurred via indirect Fe(III) mediation mechanism, rather than through electrons directly accepted from the cathode.

The reductive peak potentials shifted to more negative values with an increase in Fe(III) dosages, from 0.17 V (50 mg/L) to 0.06 V (150 mg/L), which was associated with the increase in the reductive peak currents from 4.5 A/m^2 to 16.9 A/m^2 (Fig. 5A, B and C). These results further demonstrate a decreased diffusional resistance of Cr(VI) species in the presence of increasing concentrations of Fe(III), consistent with results in Figs. 3 and 4.

ACCEPTED MANUSCRIPT

3.5 Effect of external circuital resistance

Here Fig. 6

In the presence or in the absence of Fe(III), both Cr(VI) reduction and circuital current similarly decreased as the external circuital resistance was increased (Fig. 6A and B). However, the circuital current density decreased to a greater extent than the reduction of Cr(VI), which resulted in an increase in CE_{ca} (Fig. 6C and Eq. 1). The higher CE_{ca} observed in the presence of Fe(III) rather than in its absence, at an equal external resistance, indicates that Fe(III) mediated supplementary cathodic electrons for Cr(VI) reduction. In consequence, a smaller fraction of electrons accumulated on the cathode and this resulted in higher cathode potentials at higher external resistances (Fig. 6D).

Here Fig. 7

EIS was further used to analyze the effect of external resistance on Cr(VI) reduction in the presence and in the absence of Fe(III). In the low frequency region, higher impendencies were observed at lower external resistances regardless of the presence or absence of Fe(III) (Fig. 7A and D), demonstrating that cathodic Cr(VI) reduction was controlled by diffusion resistance of this species. The presence of Fe(III) always decreased impendency at low frequencies of 0.1 – 0.01 Hz under various external resistances (Fig. 7A), implying the decreased diffusional resistance of Cr(VI) species. Low external resistance was associated with large phase angle and high electrical capacity in the presence (Fig. 7B) or absence (Fig. 7E) of Fe(III). Diminished phase angles occurred under various external resistances (Fig. 7B), compared to the situation observed in the absence of Fe(III) (Fig. 7E), stressing the

ACCEPTED MANUSCRIPT

critical role of Fe(III) in decreasing diffusional resistance of Cr(VI) species (namely no-Faraday current). The less no-Faraday current, the more favorable Cr(VI) reduction and the subsequent higher CE_{ca} (Fig. 6C).

Nyquist plots based on EIS spectra fitted to equivalent circuits (Fig. S2) were used to identify the components of the internal resistances in the cathode at different external resistances. In all cases, smaller diffusional resistance was invariably obtained in the presence of Fe(III), compared to the controls in the absence of Fe(III) (Table S1), further confirming the role of Fe(III) in decreasing diffusional resistance of Cr(VI) species.

3.6 Modeling of Cr(VI) reduction as a function of Fe(III) dose

Here Fig. 8

Table 3

Experiments at different Fe(III) dosages were performed to investigate the kinetics of Cr(VI) reduction and the reaction rate order (Fig. 8A). The results, in the presence or in the absence of Fe(III), were well described by a pseudo first-order model (Eq. 3) (Fig. 8B):

$$\ln c = k_{obs} t + \ln c_0 \quad (3)$$

with c the concentration of Cr(VI) (mg/L), k_{obs} the pseudo first-order rate constant (1/h), t the operation time (h) and c_0 the initial Cr(VI) concentration (mg/L). The slope values k_{obs} and the coefficient of determination R^2 from the linear fitting of $\ln c$ versus time are shown in Table 3. The rate constants were described as a function of Fe(III) dosage:

ACCEPTED MANUSCRIPT

$$k_{obs} = 3\times10^{-6} c_{Fe(III)}^2 + 0.001 c_{Fe(III)} + 0.125, R^2 = 0.997 \quad (4)$$

with $c_{Fe(III)}$ the Fe(III) dosage (mg/L). These modeling equations may be used to predict the concentration profile of Cr(VI) in the presence of varying Fe(III) dosages in the present MFCs.

3.7 Long-term stability

Here Fig. 9

The long-term stability of Fe(III) mediating species in the MFCs was evaluated by performing consecutive batch Cr(VI) reduction cycles using a Fe(III) dosage of 150 mg/L, and with each operational cycle extended to 10 h. The reduction of Cr(VI) marginally decreased from 98.3 ± 2.5% in the first cycle to 93.4 ± 1.6% after the tenth cycle (Fig. 9A). The circuital currents decreased from 0.29 ± 0.03 A/m^2 at 1st cycle to 0.24 ± 0.02 A/m^2 at 10th cycle (Fig. 9B) whereas the maximum power density decreased by 36% over time (Fig. 9D), mainly ascribed to the loss of Fe(III) (Fig. 9C). The loss of Fe(III) resulted from the progressive adsorption on the cationic exchange membrane separating the chambers as explained in Fig. 2D. The points of current density turning into a diffusion control regime diminished from an initial 0.28 A/m^2 to 0.22 A/m^2 at 10th cycle (Fig. 9D), implying an increase in diffusional resistance of Cr(VI) species over time. This result was in accordance with the LSV tests, where the diffusion resistance increased with the decrease in Fe(III) dosage (Fig. 3).

In summary, the comprehensive results presented in this study through multiple

ACCEPTED MANUSCRIPT

characterization methods demonstrate the significant role of Fe(III) as a mediator in MFCs for the reduction of Cr(VI) and the critical role played by Fe(III) in decreasing the diffusional resistance of Cr(VI) species and the overpotential for Cr(VI) reduction. The conversion of Cr(VI) and the CE_{ca} in the presence of Fe(III) were 1.6 times and 1.4 folds, respectively, as those recorded in its absence. In terms of Fe(III) mediating mechanism, this decreasing diffusional resistance of Cr(VI) species and the lower overpotential for Cr(VI) reduction as verified in this study, have been overlooked in previous studies [22-24]. Thus, this study provides a deeper insight into these controlling mechanisms which enhances our understanding and the performance of MFCs as an efficient technology for Cr(VI) reduction.

Practical implementation of this technology for industrial wastewater treatment requires further pilot and full-scale studies to evaluate the long-term operation and stability of the MFCs system over a feed with fluctuating characteristics and the process economics. The components with a relatively high cost in MFCs include the catalyst immobilized on the electrode and the membrane [39-41]. Although the prices of these materials are steadily decreasing [40-42], further studies are needed to raise the technology readiness level for industrial applications.

4 Conclusions

In this study, Fe(III) as an electron shuttle mediator was used for the first time to enhance the reduction of Cr(VI) in MFCs. The rate of Cr(VI) reduction reached 9.4 mg/L/h (65.6 ± 2.2%) at a Fe(III) dosage of 150 mg/L, which was 1.6-fold higher

ACCEPTED MANUSCRIPT

than the rate observed in the absence of Fe(III). The mechanism of Cr(VI) reduction primarily occurred via an indirect electron mediation by the Fe(III)/Fe(II) couple, which, in turn, further decreased both the diffusional resistance of the Cr(VI) species and the overpotential for Cr(VI) reduction. Since Fe(III) and Cr(VI) are extensively detected in the wastewaters of the electroplating and mining industries, this study provides an alternative environmentally benign approach for efficient remediation of Cr(VI) contaminated sites with simultaneous production of renewable energy.

Acknowledgments

The authors gratefully acknowledge financial support from the National Natural Science Foundation of China (Nos. 21377019 and 51578104), Specialized Research Fund for the Doctoral Program of Higher Education “SRFDP” (No. 20120041110026), and the Program for Changjiang Scholars and Innovative Research Team in University (IRT_13R05).

ACCEPTED MANUSCRIPT

References

[1] C.E. Barrera-Díaz, V. Lugo-lugo, B. Bilyeu, A review of chemical, electrochemical and biological methods for aqueous Cr(VI) reduction, J. Hazard. Mater. 223−224 (2012) 1−12. doi:10.1016/j.jhazmat.2012.04.054

[2] C. Barrera-Díaza, V. Lugo-Lugo, G. Roa-Morales, R. Natividad, S.A. Martínez-Delgadillo, Enhancing the electrochemical Cr(VI) reduction in aqueous solution, J. Hazard. Mater. 185 (2011) 1362−1368. doi:10.1016/j.jhazmat.2010.10.056

[3] Z. Li, X. Zhang, L. Lei, Electricity production during the treatment of real electroplating wastewater containing Cr(VI) using microbial fuel cell, Process Biochem. 43 (2008) 1352−1358. doi:10.1016/j.procbio.2008.08.005

[4] G. Wang, L. Huang, Y. Zhang, Cathodic reduction of hexavalent chromium Cr(VI) coupled with electricity generation in microbial fuel cells, Biotechnol. Lett. 30 (2008) 1959−1966. doi:10.1007/s10529-008-9792-4

[5] Y. Li, A. Lu, H. Ding, S. Jin, Y. Yan, C. Wang, C. Zen, X. Wang, Cr(VI) reduction at rutile-catalyzed cathode in microbial fuel cells, Electrochem. Commun. 11 (2009) 1496−1499. doi:10.1016/j.elecom.2009.05.039

[6] L. Liu, Y. Yuan, F. Li, C. Feng, In-situ Cr(VI) reduction with electrogenerated hydrogen peroxide driven by iron-reducing bacteria, Bioresour. Technol. 102 (2011) 2468−2473. doi:10.1016/j.biortech.2010.11.013

[7] B. Zhang, C. Feng, J. Ni, J. Zhang, W. Huang, Simultaneous reduction of vanadium (V) and chromium (VI) with enhanced energy recovery based on microbial fuel cell technology, J. Power Sources. 204 (2012) 34−39. doi:10.1016/j.jpowsour.2012.01.013

[8] Y. Pang, D. Xie, B. Wu, Z. Lv, X. Zeng, C. Wei, C. Feng, Conductive polymer-mediated Cr(VI) reduction in a dual-chamber microbial fuel cell under neutral conditions, Synth. Met. 183 (2013) 57−62. doi: 10.1016/j.synthmet.2013.09.019

[9] C. Choi, N. Hu, B. Lim, Cadmium recovery by coupling double microbial fuel cells, Bioresour. Technol. 170 (2014) 361−369. doi:10.1016/j.biortech.2014.07.087

[10] Y. Li, Y. Wu, S. Puranik, Y. Lei, T. Vadas, B. Li, Metals as electron acceptors in single-chamber microbial fuel cells, J. Power Sources. 269 (2014) 430−439. doi:10.1016/j.jpowsour.2014.06.117

[11] Y. Zhang, L. Yu, D. Wu, L. Huang, P. Zhou, X. Quan, Dependency of simultaneous Cr(VI), Cu(II) and Cd(II) reduction on the cathodes of microbial electrolysis cells self-driven by microbial fuel cells, J. Power Sources. 273 (2015) 1103−1113. doi:10.1016/j.jpowsour.2014.09.126

[12] L. Huang, J. Chen, X. Quan, F. Yang, Enhancement of hexavalent chromium reduction and electricity production from a biocathode microbial fuel cell,

ACCEPTED MANUSCRIPT

Bioprocess Biosyst. Eng. 33 (2010) 937−945. doi:10.1007/s00449-010-0417-7

[13] M. Tandukar, S.J. Huber, T. Onodera, S.G. Pavlostathis, Biological chromium (VI) reduction in the cathode of a microbial fuel cell, Environ. Sci. Technol. 43 (2009) 8159−8165. doi: 10.1021/es9014184

[14] E.Y. Ryu, Yeon, M. Kim, S.J. Lee, Characterization of microbial fuel cells enriched using Cr(VI)-containing sludge, J. Microbiol. Biotechnol. 21 (2011) 187−191. doi: 10.4014/jmb.1008.08019

[15] L. Huang, X. Chai, G. Chen, B.E. Logan, Effect of set potential on hexavalent chromium reduction and electricity generation from biocathode microbial fuel cells, Environ. Sci. Technol. 45 (2011) 5025−5031. doi: 10.1021/es103875d

[16] L. Huang, X. Chai, S. Cheng, G. Chen, Evaluation of carbon-based materials in tubular biocathode microbial fuel cells in terms of hexavalent chromium reduction and electricity generation, Chem. Eng. J. 166 (2011) 652−661. doi: 10.1016/j.cej.2010.11.042

[17] L. Huang, Q. Wang, L. Jiang, P. Zhou, X. Quan, B.E. Logan, Adaptively evolving bacterial communities for complete and selective reduction of Cr(VI), Cu(II), and Cd(II) in biocathode bioelectrochemical systems, Environ. Sci. Technol. 49 (2015) 9914−9924. doi: 10.1021/acs.est.5b00191

[18] L. Hsu, S.A. Masuda, K.H. Nealson, M. Pirbazari, Evaluation of microbial fuel cell *Shewanella* biocathodes for treatment of chromate contamination, RSC Advances 2 (2012) 5844−5855. doi: 10.1039/c2ra20478a

[19] N. Xafenias, Y. Zhang, C.J. Banks, Enhanced performance of hexavalent chromium reducing cathodes in the presence of *Shewanella oneidensis* MR-1 and lactate, Environ. Sci. Technol. 47 (2013) 4512−4520. doi: 10.1021/es304606u

[20] V. Sharma, P.P. Kundu, Biocatalysts in microbial fuel cells, Enzyme Microb. Technol. 47 (2010) 179−188. doi: 10.1016/j.enzmictec.2010.07.001

[21] M. Sander, T.B. Hofstetter, C.A. Gorski, Electrochemical analyses of redox-active iron minerals: A review of nonmediated and mediated approaches, Environ. Sci. Technol. 49 (2015) 5862−5878. doi: 10.1021/acs.est.5b00006

[22] A. Ter Heijne, H.V.M. Hamelers, V. De Wilde, R.A. Rozendal, C.J.N. Buisman, A bipolar membrane combined with ferric iron reduction as an efficient cathode system in microbial fuel cells, Environ. Sci. Technol. 40 (2006) 5200−5205. doi: 10.1021/es0608545

[23] A. Ter Heijne, H.V.M. Hamelers, C.J.N. Buisman, Microbial fuel cell operation with continuous biological ferrous iron oxidation of the catholyte, Environ. Sci. Technol. 41 (2007) 4130−4134. doi: 10.1021/es0702824

[24] C. Feng, F. Li, K. Sun, Y. Liu, L. Liu, X. Yue, H. Tong, Understanding the role of Fe(III)/Fe(II) couple in mediating reductive transformation of 2-nitrophenol in microbial fuel cells, Bioresour. Technol. 102 (2011) 1131−1136. doi: 10.1016/j.biortech.2010.09.005

[25] Y. Sağ, Ű. Aksu, T. Kutsal, A comparative study for the simultaneous biosorption of Cr(VI) and Fe(III) on *C. vulgaris* and *R. arrhizus*: Application of the competitive adsorption models, Process Biochem 33 (1998) 273-281.

ACCEPTED MANUSCRIPT

doi:10.1016/S0032-9592(97)00060-5
[26] P. Clauwaert, P. Aelterman, T.H. Pham, L. De Schamphelaire, M. Carballa, K. Rabaey, W. Verstraete, Minimizing losses in bio-electrochemical systems: The road to applications, Appl. Microbiol. Biotechnol. 79 (2008) 901−913. doi: 10.1007/s00253-008-1522-2
[27] D. Ki, S.C. Popat, C.I. Torres, Reduced overpotentials in microbial electrolysis cells through improving design, operation, and electrochemical characterization, Chem. Eng. J. 287 (2016) 181−188. doi: 10.1016/j.cej.2015.11.022
[28] R. Burkitt, T.R. Whiffen, E.H. Yu, Iron phthalocyanine and MnOx composite catalysts for microbial fuel cell applications, Appl. Catalysis B-Environ. 181 (2016) 279−288. doi: 10.1016/j.apcatb.2015.07.010
[29] Y. Yuan, Y. Jeon, J. Ahmed, W. Park, S. Kim, Use of carbon nanoparticles for bacteria immobilization in microbial fuel cells for high power output, J. Electrochem. Soc. 156 (2009) B1238−1241. doi: 10.1149/1.3190477
[30] J. Sun, Y.Y. Hu, B. Hou, Electrochemical characteriztion of the bioanode during simultaneous azo dye decolorization and bioelectricity generation in an air-cathode single chambered microbial fuel cell, Electrochim. Acta 56 (2011) 6874−6879. doi: 10.1016/j.electacta.2011.05.111
[31] Y. Liu, J. Shen, L. Huang, D. Wu, Copper catalysis for enhancement of cobalt leaching and acid utilization efficiency in microbial fuel cells, J. Hazard. Mater. 262 (2013) 1−8. doi:10.1016/j.jhazmat.2013.08.004.
[32] D. Wu, L. Huang, X. Quan, G. Li Puma. Electricity generation and bivalent copper reduction as a function of operation time and cathode electrode material in microbial fuel cells, J. Power Sources 307 (2016) 705−714. doi: 10.1016/j.jpowsour.2016.01.022
[33] Q. Wang, L. Huang, H. Yu, X. Quan, Y. Li, G. Fan, L. Li, Assessment of five different cathode materials for Co(II) reduction with simultaneous hydrogen evolution in microbial electrolysis cells, Inter. J. Hydrogen Energy 40 (2015) 184−196. doi: 10.1016/j.ijhydene.2014.11.014
[34] S. Cheng, D. Xing, D.F. Call, B.E. Logan, Direct biological conversion of electrical current into methane by electromethanogenesis, Environ. Sci. Technol. 43 (2009) 3953−3958. doi: 10.1021/es803531g
[35] American Public Health Association, American Water Works Association, Water Pollution Control Federation (1998) Standard methods for the examination of water and wastewater, 20th edn. American Public Health Association, Washington, DC.
[36] S. Freguia, K. Rabaey, Z. Yuan, Non-catalyzed cathodic oxygen reduction at graphite granules in microbial fuel cells, Electrochem. Acta. 53 (2007) 598−603. doi:10.1016/j.electacta.2007.07.037.
[37] F. Zhao, R.C.T. Slade, J.R. Varcoe, Techniques for the study and development of microbial fuel cells : An electrochemical perspective, Chem. Soc. Rev. 38 (2009) 1926−1939. doi:10.1039/b819866g.
[38] F. Zhao, F. Harnisch, U. Schroder, F. Scholz, P. Bogdanoff, I. Herrmann, Challenges and constraints of using oxygen cathodes in microbial fuel,

ACCEPTED MANUSCRIPT

Environ. Sci. Technol. 40 (2006) 5193−5199. doi**:** 10.1021/es060332p

[39] D. Pant, A. Singh, G. Van Bogaert, Y. A. Gallego, L. Diels, K. Vanbroekhoven. An introduction to the life cycle assessment (LCA) of bioelectrochemical systems (BES) for sustainable energy and product generation: Relevance and key aspects, Renew Sust Energy Rev 15 (2011) 1305-1313. doi: 10.1016/j.rser.2010.10.005

[40] J. Wei, P. Liang, X. Huang, Recent progress in electrodes for microbial fuel cells, Bioresour. Technol. 102 (2011) 9335-9344. doi: 10.1016/j.biortech.2011.07.019

[41] W. Li, H. Yu, Z. He, Towards sustainable wastewater treatment by using microbial fuel cells-centered technologies, Energy Environ. Sci. 7 (2014) 911-924. doi: 10.1039/C3EE43106A

[42] X. Liu, W. Li, H. Yu, Cathodic catalysts in bioelectrochemical systems for energy recovery from wastewater, Chem. Soc. Rev. 43 (2014) 7718-7745. doi: 10.1039/c3cs60130g

ACCEPTED MANUSCRIPT

Figure and Table legends

Fig. 1 Reduction of Cr(VI) via either indirect electron transfer of Fe(III) mediation or direct electron transfer between cathode electrode and final electron acceptor of Cr(VI).

Fig. 2 (A) Cr(VI) reduction, (B) current density, (C) CE_{ca}, and (D) loss of Fe(III) as a function of Fe(III) dosage in MFCs after 3 hours of operation.

Fig. 3 (A) Voltage output, (B) power density, and (C) cathode and anode potentials under various Fe(III) dosages as a function of current density.

Fig. 4 Tafel plots of (A) log current density vs. cathodic potential, and (B) cathodic overpotential vs. log current density for the estimation of Tafel slop and exchange current for Cr(VI) reduction at various Fe(III) dosages.

Fig. 5 Comparison of CVs in catholytes at Fe(III) dosages of (A) 50 mg/L, (B) 100 mg/L and (C) 150 mg/L.

Fig. 6 Effect of external resistance on (A) Cr(VI) reduction, (B) circuital current, (C) cathode potential, and (D) CE_{ca} in the presence or absence of Fe(III).

Fig.7 Comparison of EIS spectra for the cathode at different cathodic potentials corresponding to various external resistance in the (A, B and C) presence or (D, E and F) absence of Fe(III) using (A and D) logarithm of impendence modulus, (B and E) phase angle versus the logarithm of frequency, and (C and F) nyquist plots.

Fig. 8 Time course of (A) Cr(VI) reduction and (B) Ln Cr(VI) concentration in the presence of various Fe(III) dosages.

Fig. 9 (A) Cr(VI) reduction, (B) current density, (C) Fe(III) concentration vs. number of cycle, and (D) polarization curves at the 1^{st} and 10^{th} cycle.

ACCEPTED MANUSCRIPT

Tables

ACCEPTED MANUSCRIPT

Table 1 Summery of literature on Cr(VI) reduction in MFCs.

Reactor	Cr(VI) reduction site	Electrode material	Mediator	Initial Cr(VI) (mg/L)	Initial pH	Operation time (h)	External resistor (Ω)	Cr(VI) removal rate (mg/L/h)	Cr(VI) removal (%)	References
two chamber	abiotic cathode	graphite paper	none	50	2.0	9	1000	5.46	98	[3]
two chamber	abiotic cathode	graphite plate	none	100	2.0	150	1000	0.67	100	[4]
		carbon paper						4.79	86	
		carbon felt						2.26	41	
two chamber	abiotic cathode	graphite	rutile	26	2.0	22	5000	1.04	88	[5]
			none					0.77	65	
two chamber	abiotic cathode	carbon felt	H_2O_2	10	2.0	4	500	2.50	100	[6]
			none			12		0.35	43	
two chamber	abiotic cathode	carbon fiber	none	250	2.0	240	1000	0.79	75	[7]
two chamber	abiotic cathode	graphite felt	pyrrole/ClO_4^-	20	7.0	46	300	0.37	85	[8]
			pyrrole/anthraquinone-2-sulfonate					0.44	100	
			none					0.14	33	
two chamber	abiotic cathode	carbon cloth	none	200	2.0	60	none	0.47	14	[9]

ACCEPTED MANUSCRIPT

single chamber	abiotic cathode	carbon cloth	mixed culture	10	6.5	120	500	0.08	99	[10]
two chamber	abiotic cathode	carbon rod	none	50	2	4	1000	4.28	34	[11]
two chamber	biotic cathode	granule graphite	mixed culture	39	7.0	7	1000	5.6	100	[12]
two chamber	biotic cathode	graphite plate	mixed culture	63	7.2-7.6	120	1000	0.53	100	[13]
two chamber	biotic anode	graphite felt	mixed culture	5	none	none	200	none	93	[14]
				25				none	61	
two chamber	biotic cathode	carbon fiber	mixed culture	20	7.0	5	400	3.60	90	[15]
		carbon granule						3.46	87	
		carbon felt						3.07	77	
two chamber	biotic cathode	graphite granule	mixed culture	20	7.0	24	set potential	0.82	99	[16]
							200	0.42	50	
two chamber	biotic cathode	graphite felt	mixed culture	5	5.8	4	510	1.24	100	[17]
two chamber	biotic cathode	reticulated vitreous carbon	*Shewanella*	2.6	7.0	72	10	0.03	100	[18]
two chamber	biotic cathode	graphite felt	*Shewanella*	20	7	4	1000	2.25	45	[19]

ACCEPTED MANUSCRIPT

Table 2 Values of Tafel slopes and exchange currents for Cr(VI) reduction at various Fe(III) dosages.

Fe(III) dosage (mg/L)	0	50	100	150
Tafel slope (mV/(decade A/m^2))	89.9	82.2	76.9	68.9
β	0.29	0.31	0.33	0.37
Exchange current (A/m^2)	2.70×10^{-3}	3.22×10^{-3}	4.02×10^{-3}	4.60×10^{-3}

ACCEPTED MANUSCRIPT

Table 3 Pseudo-first-order reaction rate constants and correlation coefficients for Cr(VI) reduction at various Fe(III) dosages in MFCs.

Fe(III) dosage (mg/L)	0	25	50	75	100	125	150
Rate constant k (h^{-1})	0.127	0.148	0.180	0.207	0.247	0.292	0.322
R^2	0.991	0.996	0.993	0.997	0.990	0.995	0.993

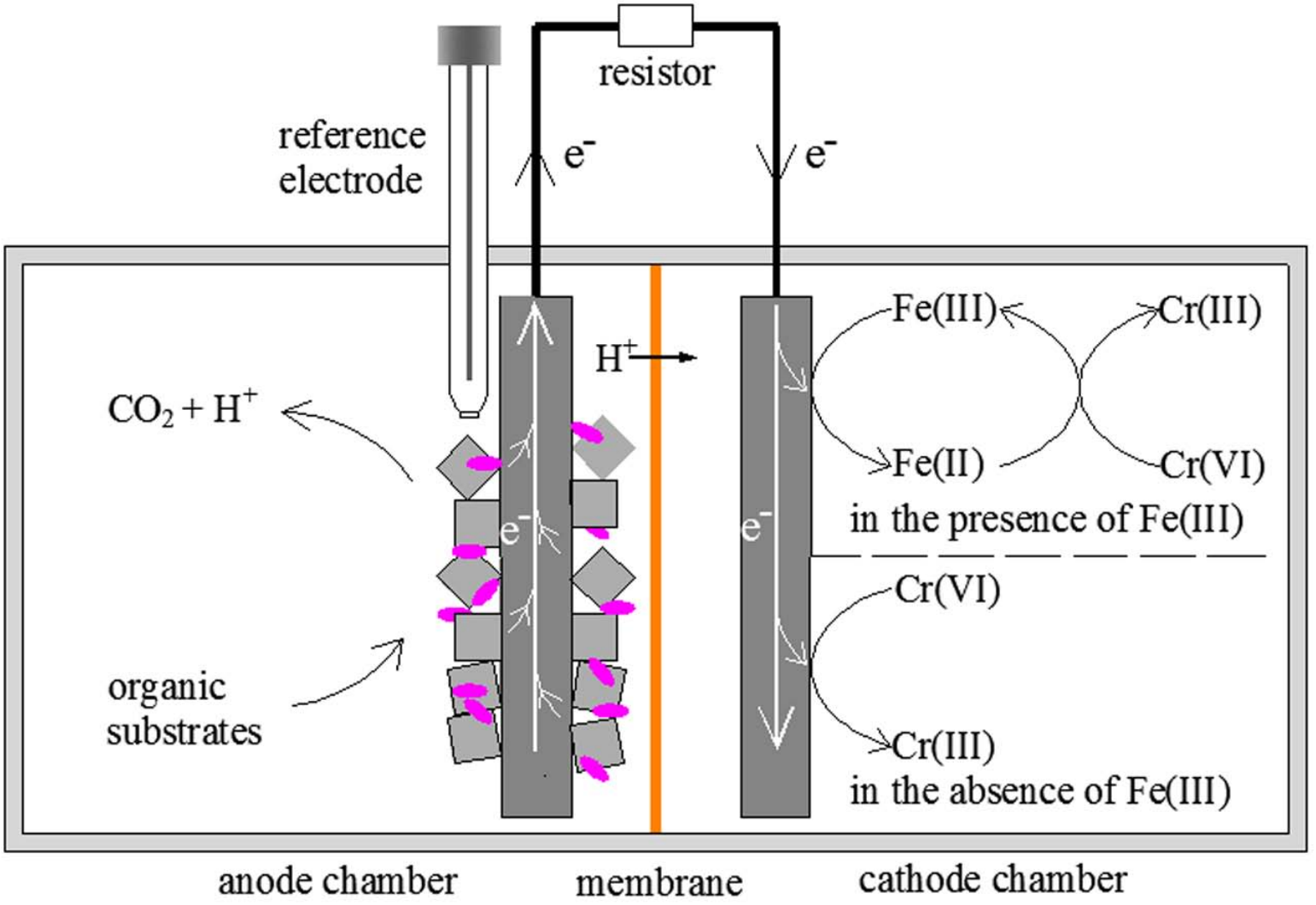
resistor
reference electrode
e-
e-
H+
CO2 + H+
e-
e-
Fe(III)
Cr(III)
Fe(II)
Cr(VI)
in the presence of Fe(III)
Cr(VI)
organic substrates
Cr(III)
in the absence of Fe(III)
anode chamber
membrane
cathode chamber

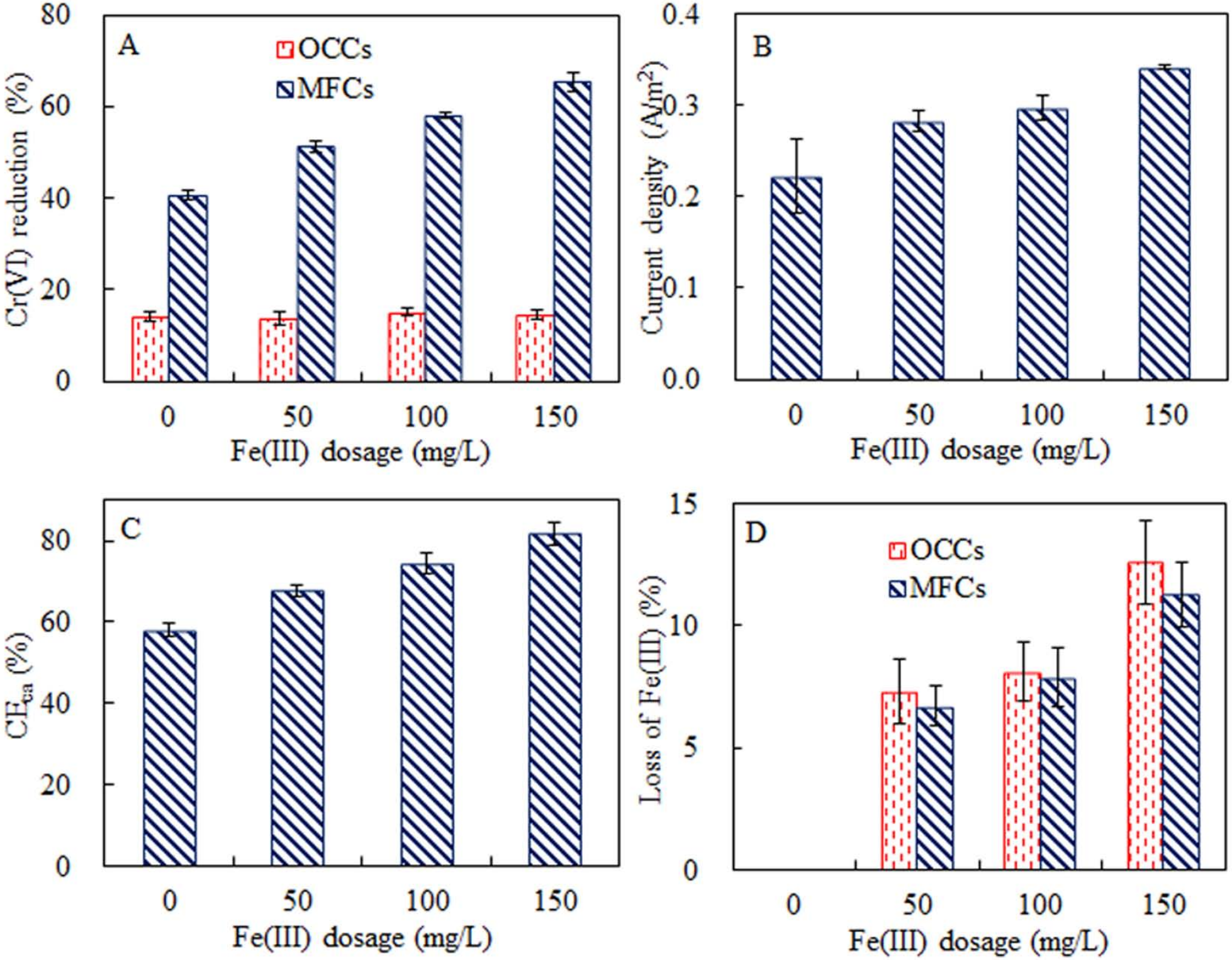
A
OCCs
MFCs
Cr(VI) reduction (%)
0
20
40
60
80
0
50
100
150
Fe(III) dosage (mg/L)
B
Current density (A/m²)
0.0
0.1
0.2
0.3
0.4
0
50
100
150
Fe(III) dosage (mg/L)
C
CE_ca (%)
0
20
40
60
80
0
50
100
150
Fe(III) dosage (mg/L)
D
OCCs
MFCs
Loss of Fe(III) (%)
0
5
10
15
0
50
100
150
Fe(III) dosage (mg/L)

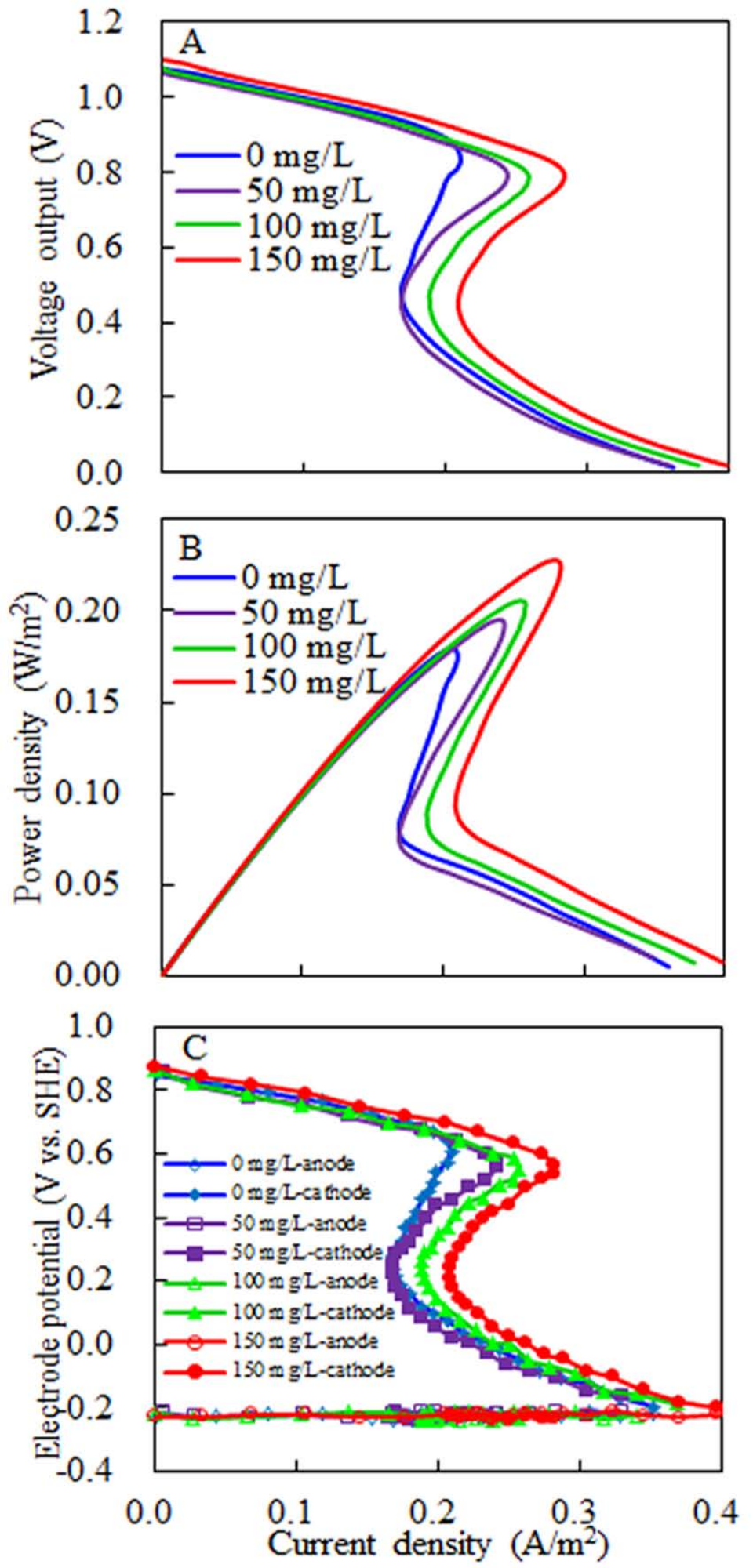
A
Voltage output (V)
1.2
1.0
0.8
0.6
0.4
0.2
0.0
0 mg/L
50 mg/L
100 mg/L
150 mg/L
B
Power density (W/m2)
0.25
0.20
0.15
0.10
0.05
0.00
0 mg/L
50 mg/L
100 mg/L
150 mg/L
C
Electrode potential (V vs. SHE)
1.0
0.8
0.6
0.4
0.2
0.0
-0.2
-0.4
0 mg/L-anode
0 mg/L-cathode
50 mg/L-anode
50 mg/L-cathode
100 mg/L-anode
100 mg/L-cathode
150 mg/L-anode
150 mg/L-cathode
0.0
0.1
0.2
0.3
0.4
Current density (A/m2)

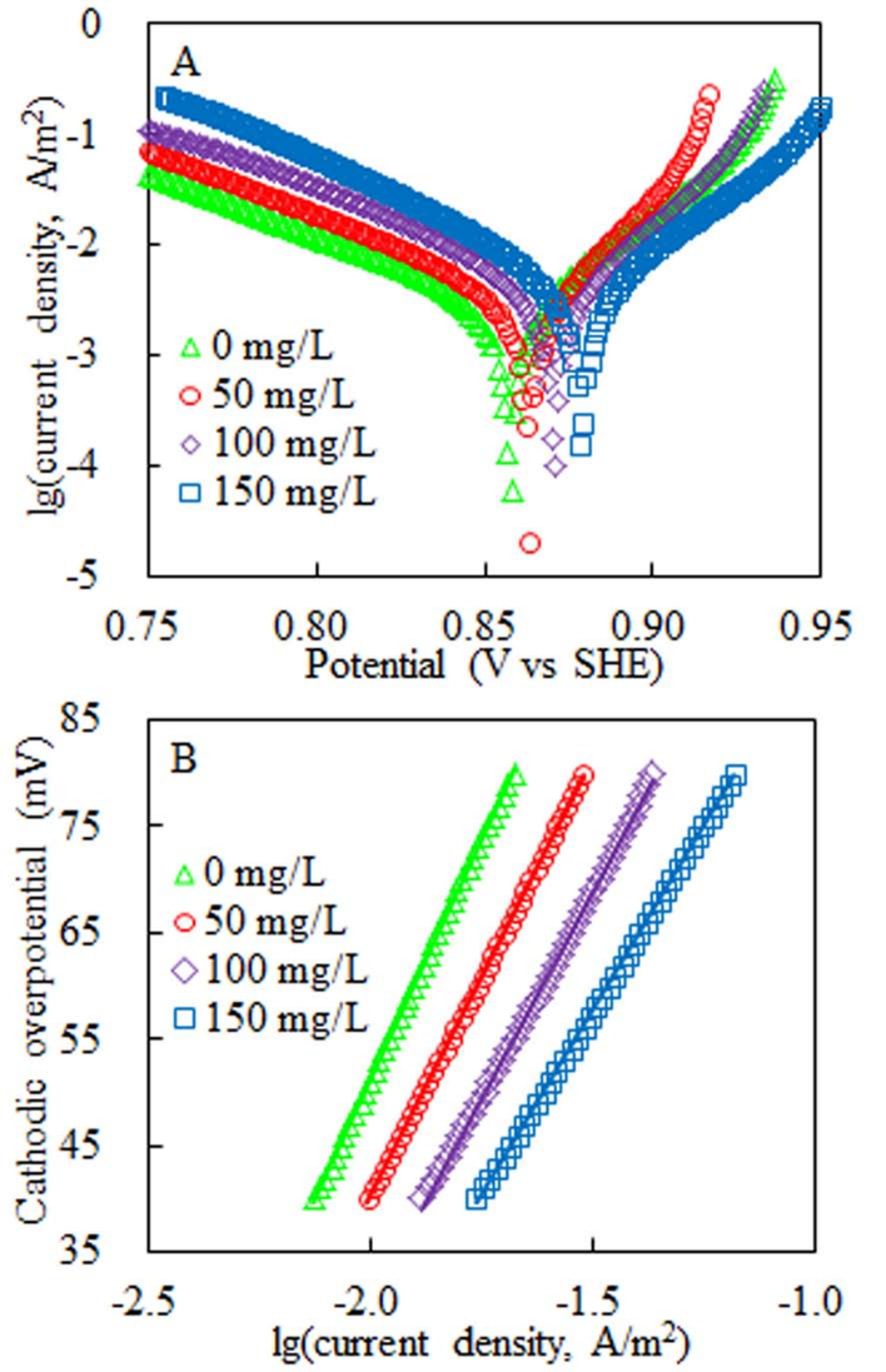
A
0 mg/L
50 mg/L
100 mg/L
150 mg/L
lg(current density, A/m²)
Potential (V vs SHE)
0
-1
-2
-3
-4
-5
0.75
0.80
0.85
0.90
0.95
B
0 mg/L
50 mg/L
100 mg/L
150 mg/L
Cathodic overpotential (mV)
lg(current density, A/m²)
85
75
65
55
45
35
-2.5
-2.0
-1.5
-1.0

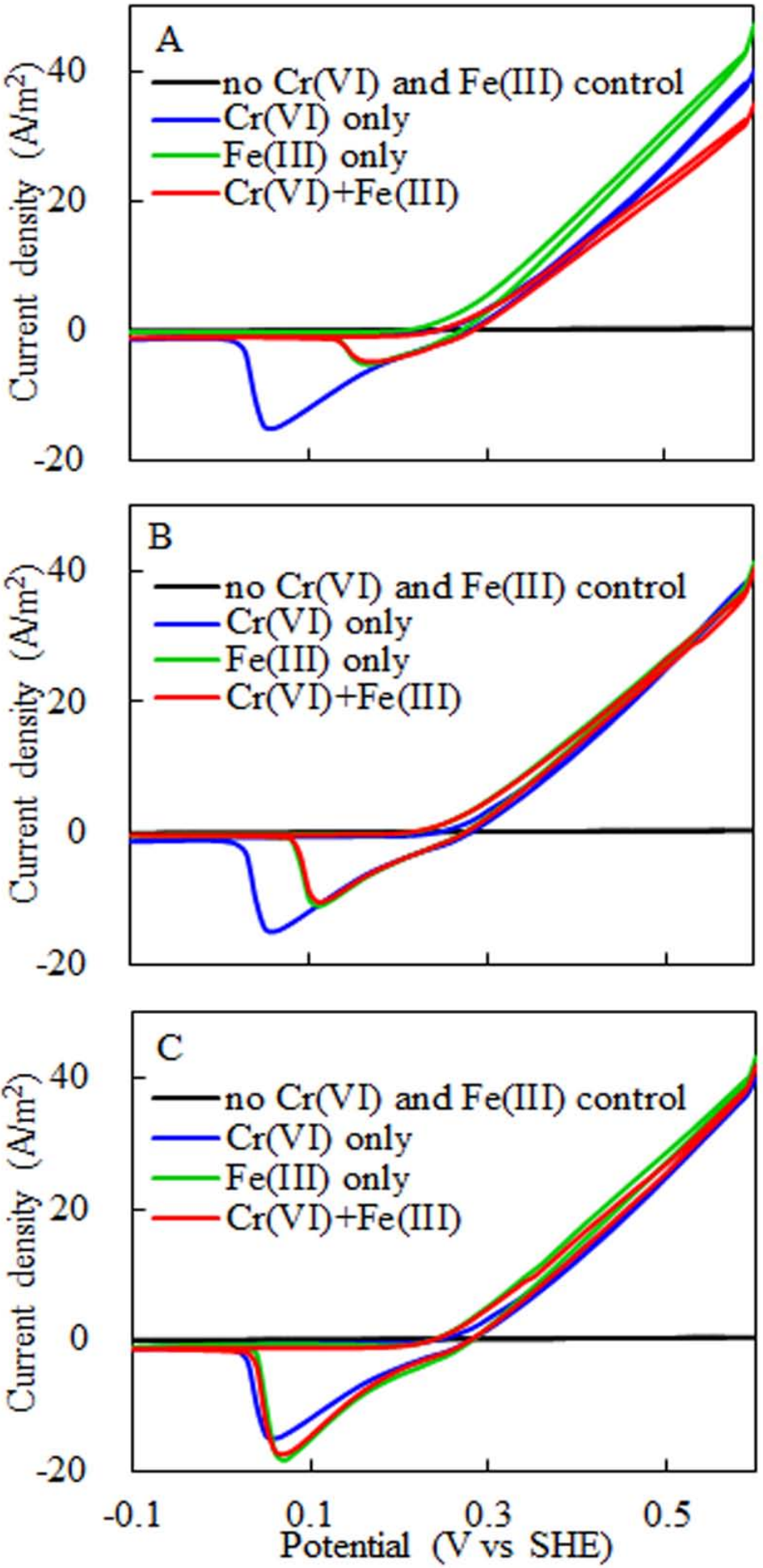
A
no Cr(VI) and Fe(III) control
Cr(VI) only
Fe(III) only
Cr(VI)+Fe(III)
Current density (A/m²)
40
20
0
-20
B
no Cr(VI) and Fe(III) control
Cr(VI) only
Fe(III) only
Cr(VI)+Fe(III)
Current density (A/m²)
40
20
0
-20
C
no Cr(VI) and Fe(III) control
Cr(VI) only
Fe(III) only
Cr(VI)+Fe(III)
Current density (A/m²)
40
20
0
-20
-0.1
0.1
0.3
0.5
Potential (V vs SHE)

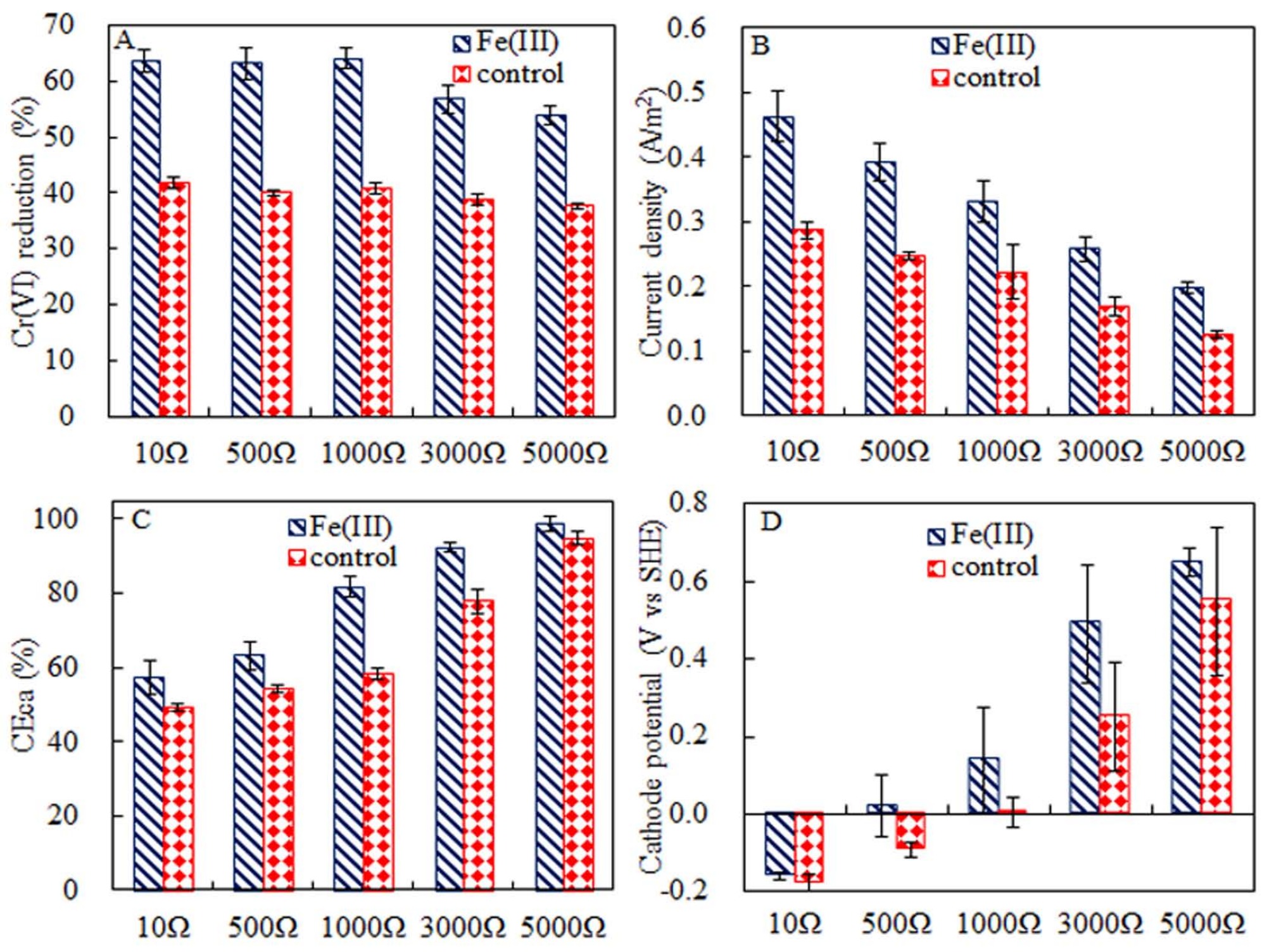
A
Fe(III)
control
Cr(VI) reduction (%)
0
10
20
30
40
50
60
70
10Ω
500Ω
1000Ω
3000Ω
5000Ω
B
Fe(III)
control
Current density (A/m²)
0.0
0.1
0.2
0.3
0.4
0.5
0.6
10Ω
500Ω
1000Ω
3000Ω
5000Ω
C
Fe(III)
control
CEca (%)
0
20
40
60
80
100
10Ω
500Ω
1000Ω
3000Ω
5000Ω
D
Fe(III)
control
Cathode potential (V vs SHE)
-0.2
0.0
0.2
0.4
0.6
0.8
10Ω
500Ω
1000Ω
3000Ω
5000Ω

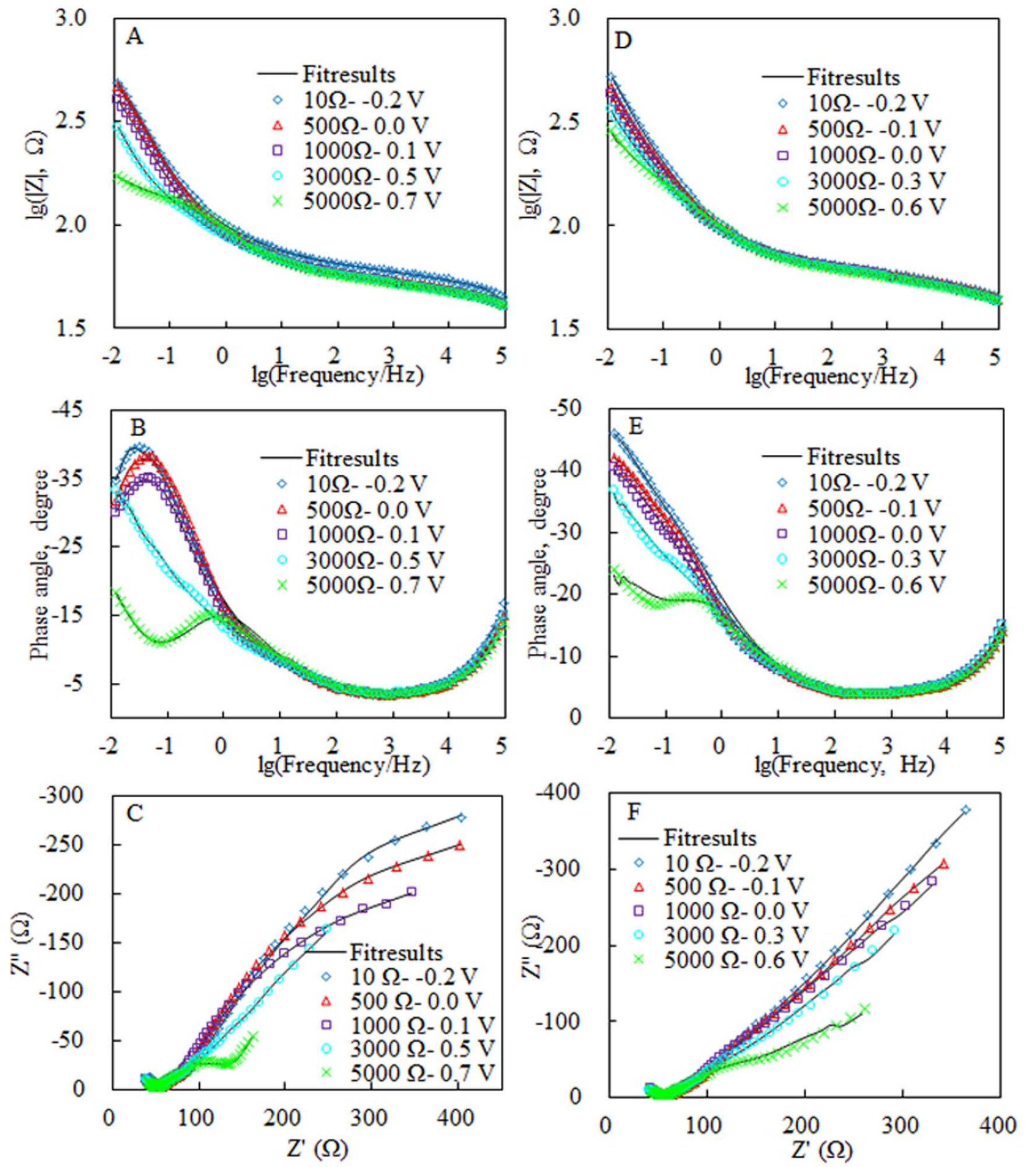
A
Fitresults
10Ω- -0.2 V
500Ω- 0.0 V
1000Ω- 0.1 V
3000Ω- 0.5 V
5000Ω- 0.7 V
lg(|Z|, Ω)
lg(Frequency/Hz)
D
Fitresults
10Ω- -0.2 V
500Ω- -0.1 V
1000Ω- 0.0 V
3000Ω- 0.3 V
5000Ω- 0.6 V
lg(|Z|, Ω)
lg(Frequency/Hz)
B
Fitresults
10Ω- -0.2 V
500Ω- 0.0 V
1000Ω- 0.1 V
3000Ω- 0.5 V
5000Ω- 0.7 V
Phase angle, degree
lg(Frequency/Hz)
E
Fitresults
10Ω- -0.2 V
500Ω- -0.1 V
1000Ω- 0.0 V
3000Ω- 0.3 V
5000Ω- 0.6 V
Phase angle, degree
lg(Frequency, Hz)
C
Fitresults
10 Ω- -0.2 V
500 Ω- 0.0 V
1000 Ω- 0.1 V
3000 Ω- 0.5 V
5000 Ω- 0.7 V
Z'' (Ω)
Z' (Ω)
F
Fitresults
10 Ω- -0.2 V
500 Ω- -0.1 V
1000 Ω- 0.0 V
3000 Ω- 0.3 V
5000 Ω- 0.6 V
Z'' (Ω)
Z' (Ω)

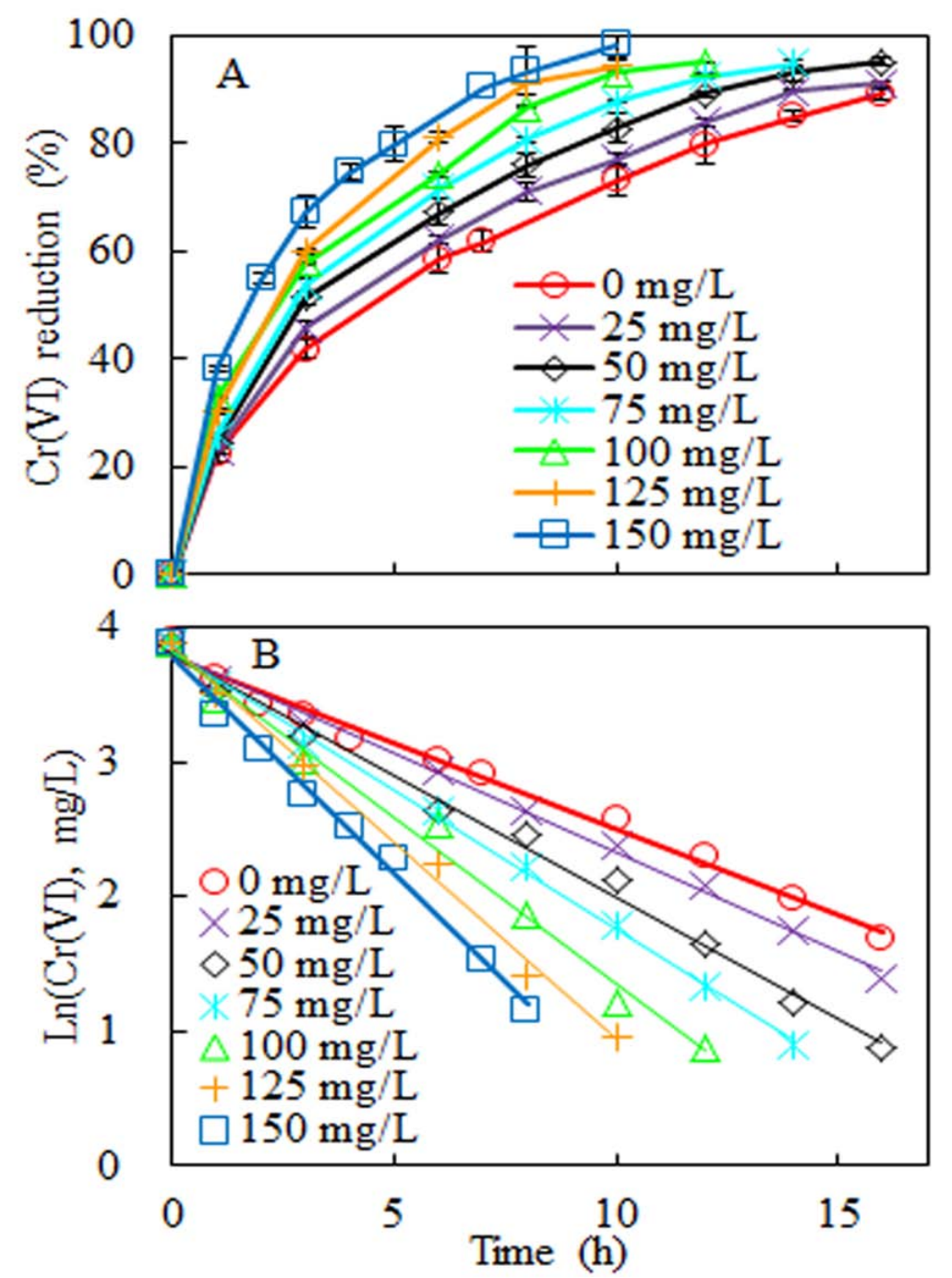
A
Cr(VI) reduction (%)
100
80
60
40
20
0
0 mg/L
25 mg/L
50 mg/L
75 mg/L
100 mg/L
125 mg/L
150 mg/L
B
Ln(Cr(VI), mg/L)
4
3
2
1
0
0 mg/L
25 mg/L
50 mg/L
75 mg/L
100 mg/L
125 mg/L
150 mg/L
0
5
10
15
Time (h)

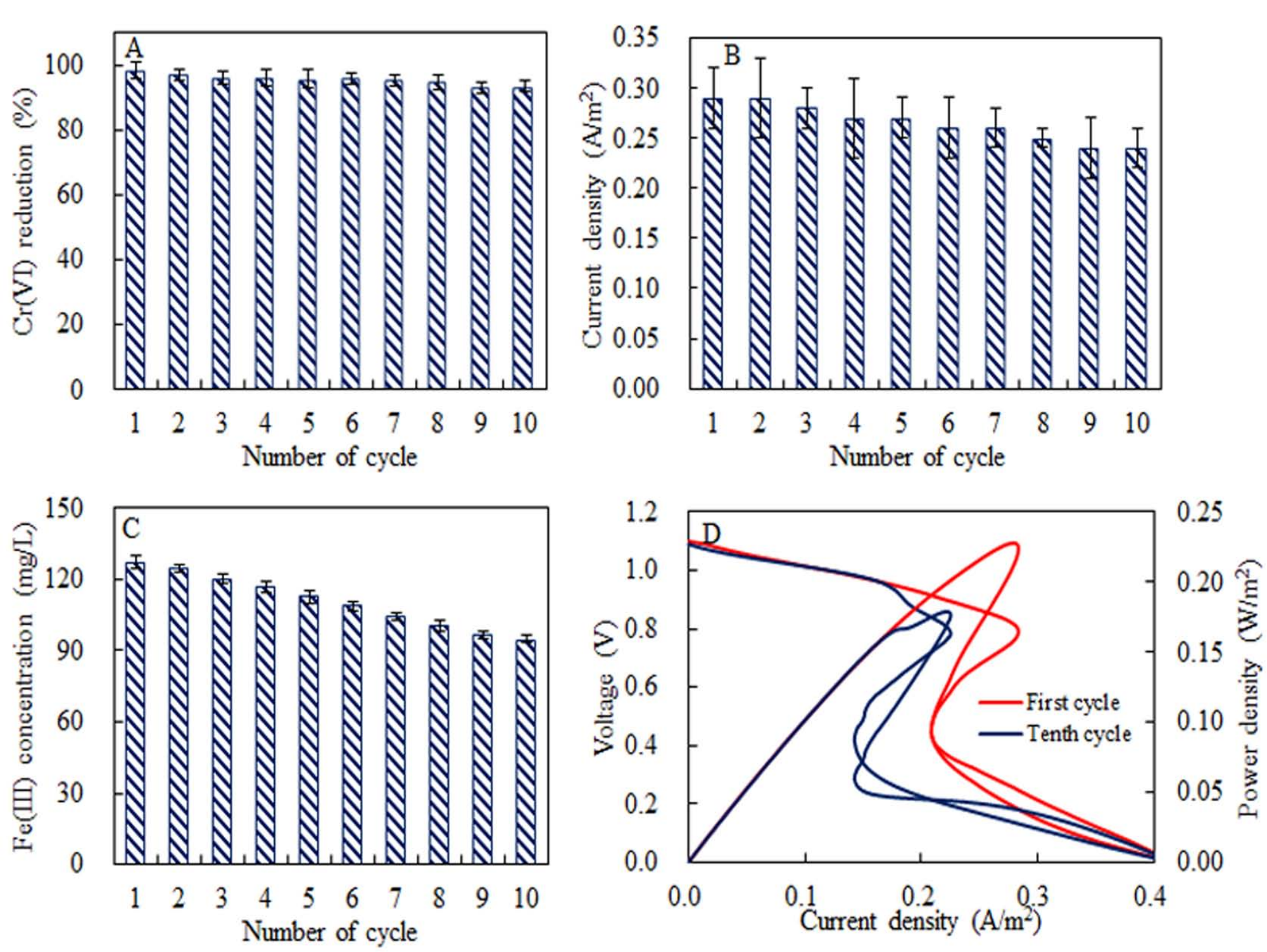
A
Cr(VI) reduction (%)
Number of cycle
B
Current density (A/m²)
Number of cycle
C
Fe(III) concentration (mg/L)
Number of cycle
D
Voltage (V)
Power density (W/m²)
Current density (A/m²)
First cycle
Tenth cycle